



HAL
open science

The Amnesic Shellfish Poisoning toxin, domoic acid: the tattoo of the king scallop *Pecten maximus*

José Luis García-Corona, Caroline Fabioux, Jean Vanmaldergem, Sylvain Petek, Amélie Derrien, Aouregan Terre-Terrillon, Laura Bressolier, Florian Breton, Hélène Hegaret

► To cite this version:

José Luis García-Corona, Caroline Fabioux, Jean Vanmaldergem, Sylvain Petek, Amélie Derrien, et al.. The Amnesic Shellfish Poisoning toxin, domoic acid: the tattoo of the king scallop *Pecten maximus*. Harmful Algae, 2024, 133, pp.102607. 10.1016/j.hal.2024.102607 . hal-04487905

HAL Id: hal-04487905

<https://hal.univ-brest.fr/hal-04487905>

Submitted on 4 Mar 2024

HAL is a multi-disciplinary open access archive for the deposit and dissemination of scientific research documents, whether they are published or not. The documents may come from teaching and research institutions in France or abroad, or from public or private research centers.

L'archive ouverte pluridisciplinaire **HAL**, est destinée au dépôt et à la diffusion de documents scientifiques de niveau recherche, publiés ou non, émanant des établissements d'enseignement et de recherche français ou étrangers, des laboratoires publics ou privés.

1 **The Amnesic Shellfish Poisoning toxin, domoic acid: the tattoo of the king scallop *Pecten***
2 ***maximus***

3

4 José Luis García-Corona¹, Caroline Fabioux¹, Jean Vanmaldergem¹, Sylvain Petek¹, Amélie
5 Derrien², Aouregan Terre-Terrillon², Laura Bressolier¹, Florian Breton³ & Hélène Hegaret^{1*}

6

7 ¹Institut Universitaire Européen de la Mer, Laboratoire des Sciences de l'Environnement
8 Marin, UMR 6539 LEMAR UBO, CNRS, IRD, Ifremer, F-29280 Plouzané, France.

9

10 ²Ifremer, LITTORAL LER BO, Station de Biologie Marine, Place de la Croix, BP40537,
11 29900 Concarneau Cedex, France.

12

13 ³Écloserie du Tinduff, 148 rue de l'écloserie, Port du Tinduff, 29470, Plougastel-Daoulas,
14 France.

15

16 *Corresponding author: Hélène Hegaret

17

18 Institut Universitaire Européen de la Mer, Laboratoire des Sciences de l'Environnement
19 Marin, UMR 6539 LEMAR UBO, CNRS, IRD, Ifremer, F-29280 Plouzané, France.

20

21 e-mail: helene.hegaret@univ-brest.fr

22 **Abstract**

23 Domoic acid (DA) is a potent neurotoxin produced by diatoms of the genus *Pseudo-nitzschia*
24 and is responsible for Amnesic Shellfish Poisoning (ASP) in humans. Some fishery resources
25 of high commercial value, such as the king scallop *Pecten maximus*, are frequently exposed to
26 toxic *Pseudo-nitzschia* blooms and are capable of accumulating high amounts of DA,
27 retaining it for months or even a few years. This poses a serious threat to public health and a
28 continuous economical risk due to fishing closures of this resource in the affected areas.
29 Recently, it was hypothesized that trapping of DA within autophagosomic-vesicles could be
30 one reason explaining the long retention of the remaining toxin in *P. maximus* digestive gland.
31 To test this idea, we follow the kinetics of the subcellular localization of DA in the digestive
32 glands of *P. maximus* during (a) the contamination process — with sequential samplings of
33 scallops reared in the field during 234 days and naturally exposed to blooms of DA-producing
34 *Pseudo-nitzschia australis*, and (b) the decontamination process — where highly
35 contaminated scallops were collected after a natural bloom of toxic *P. australis* and subjected
36 to DA-depuration in the laboratory for 60 days. In the digestive gland, DA-depuration rate
37 (0.001 day^{-1}) was much slower than contamination kinetics. The subcellular analyses revealed
38 a direct implication of early autophagy in DA sequestration throughout contamination ($r =$
39 0.8 , $P < 0.05$), while the presence of DA-labeled residual bodies (late autophagy) appeared to
40 be strongly and significantly related to slow DA-depuration ($r = -0.5$) resembling an
41 analogous DA-tattooing in the digestive glands of *P. maximus*. This work provides new
42 evidence about the potential physiological mechanisms involved in the long retention of DA
43 in *P. maximus* and represents the baseline to explore procedures to accelerate decontamination
44 in this species.

45 **Keywords:** domoic acid, *Pecten maximus*, toxicokinetics, rapid accumulation, slow
46 depuration, autophagy.

47

48 1. Introduction

49 Over the last three decades, natural stocks of important fishery resources have been subjected
50 to intense and frequent blooms of toxic diatoms of the genus *Pseudo-nitzschia*, widely
51 distributed throughout all oceans of the world (Hallegraeff 1993; Lelong *et al.*, 2012; Trainer
52 *et al.*, 2012). To date, about 28 species of this genus have been reported to be capable of
53 producing domoic acid (DA), an extremely dangerous amino acid responsible for Amnesic
54 Shellfish Poisoning (ASP) in mammals (Pulido, 2008; La Barre *et al.*, 2014; Bates *et al.*,
55 2018). The species *P. australis* is frequently reported as one of the most toxigenic of all (Basti
56 *et al.*, 2018; Ayache *et al.*, 2019) and in recent years, its presence has been detected in several
57 countries around the world (Lelong *et al.*, 2012; Bates *et al.*, 2018) including on the northwest
58 coast of France. This represents a threat to the fishing-aquaculture industry due to the
59 numerous persistent harvest closures of shellfish beds (Amzil *et al.*, 2001; Husson *et al.*,
60 2016; Ayache *et al.*, 2019).

61 The European Union 2002/226/EC banned shellfish harvesting when DA concentrations
62 exceed the sanitary limit of 20 mg. kg⁻¹ of flesh on the whole or individual parts of shellfish
63 (MacKenzie *et al.*, 2002; Wekel *et al.*, 2004) to avoid public health issues. The king scallop
64 *Pecten maximus* is a very valuable fishery resource in the western coast of Europe. In France,
65 this species has an important economic and commercial value (~ 87 million euros yearly);
66 however, the recurrent proliferations of DA-producing *Pseudo-nitzschia* and the subsequent
67 re intoxication episodes of the natural stocks of these resources (Amzil *et al.*, 2001; Husson *et*
68 *al.*, 2016; Ayache *et al.*, 2019) have led to severe economic losses of nearly 70 million euros
69 per year due to fishery closures (France Filière Pêche: <https://www.francefilierepeche.fr/>).
70 King scallops have been reported to accumulate less than 6% of total DA burdens in the joint
71 of soft tissues like adductor muscle, gonad, kidney, gills, and mantle, and amounts as high as
72 3,200 mg. DA kg⁻¹ in the digestive gland (> 80% of the total DA) retaining it from several
73 months to even a few years (Blanco *et al.*, 2002a, 2006, 2020). Therefore, the European
74 decision 91/492/EEC allowed the commercialization of *P. maximus* after evisceration of the
75 inedible tissues (i.e. the digestive gland) to reduce the toxin contents (< 4.6 mg. DA kg⁻¹ in
76 muscle and gonad) in authorized processing plants.

77 Many bivalves depurate the toxin quickly, showing decontamination rates of up to 10 day⁻¹ in
78 digestive tissues, like some mussels (Wohlgeschaffen *et al.*, 1992; Novaczek *et al.*, 1992;
79 Blanco *et al.*, 2002b; Mafra *et al.*, 2010; Bresnan *et al.*, 2017), clams (Gilgan *et al.*, 1990;

80 Blanco *et al.*, 2010; Álvarez *et al.*, 2015; Dusek Jennings *et al.*, 2020), and oysters (Jones *et al.*, 1995; Mafra *et al.*, 2010). Some scallops such as *Argopecten purpuratus* are also capable
81 of excreting up to $\geq 80\%$ of total DA-burdens in a few hours, and $\sim 90\%$ in a couple of days
82 (Álvarez *et al.*, 2020). On the contrary, other bivalves exhibit slow toxin excretion rates ≤ 0.3
83 day^{-1} in the digestive gland, as reported for the razor clam *Siliqua patula* (Drum *et al.*, 1993;
84 Horner *et al.*, 1993; Dusek Jennings *et al.*, 2020). Nevertheless, some scallops such as
85 *Placopecten magellanicus* (Wohlgeschaffen *et al.*, 1992; Douglas *et al.*, 1997), and *P.*
86 *maximus* (Blanco *et al.*, 2002a 2006; Mauríz & Blanco, 2010; Bresnan *et al.*, 2017) show the
87 slowest DA-decontamination kinetics, with rates as slow as 0.05 to 0.007 day^{-1} , respectively,
88 in the digestive gland. It thus appears necessary to better understand the mechanisms
89 associated with this long DA retention.
90

91 Physiological mechanisms behind the broad interspecific differences in accumulation and
92 depuration dynamics of DA are still not fully understood. Mauriz and Blanco (2010)
93 suggested that the absence of efficient membrane transporters to excrete the toxin could
94 explain the high accumulation and/or slow depuration of DA in *P. maximus*. Meanwhile, in *A.*
95 *purpuratus*, the key to the accelerated depuration rates of the toxin could rely on the rapid
96 transfer of most of DA burdens accumulated in the digestive gland to other organs capable to
97 excrete it with greater efficacy (Álvarez *et al.*, 2020). Other mechanisms, such as the
98 expression of low affinity glutamate receptors in all tissues, and the selective activation of
99 high DA capacity sites in tissues such as siphon have been proposed as an explanation for the
100 tissue-specific long retention of ASP toxins in species like *S. patula* (Trainer and Bill, 2004).

101 Recently, Garcia-Corona *et al.* (2022; 2024) observed, thanks to an immunostaining of DA,
102 that in species like *P. maximus*, *Aequipecten opercularis* (queen scallop), and *Crepidula*
103 *fornicata* (slipper-limpet), most of the DA staining was trapped within small ($\sim 1\text{-}2.5 \mu\text{m}$)
104 autophagic vesicles in the cytoplasm of the digestive cells during active digestion (early
105 autophagy), as well as in remaining post-digestion residual bodies in the distal cytoplasmic
106 zone of digestive cells, undergoing advanced digestion (late autophagy). Nevertheless, none
107 of these hypotheses has been fully elucidated so far. Autophagy is a highly organized and
108 complex intracellular catabolic degradation system well conserved in eukaryotic cells (Owen,
109 1972, Wang *et al.*, 2019; Zhao *et al.*, 2021). Through this process, the own (*e.g.*, abnormal
110 proteins, excess or damaged organelles) or foreign (*e.g.*, pathogenic microorganisms,
111 chemical compounds) cytoplasmic contents of the cell are digested to recycle energy usable
112 by the cell, or processed for its cell excretion, respectively (Cuervo, 2004; Zheng *et al.*, 2022).

113 The key structures in autophagy are autophagosomes, spherical vesicles from 0.5 to 2.5 μm in
114 diameter with a double phospholipid membrane (Mizushima *et al.*, 2002). The essential role
115 of autophagy is a key piece in the maintenance of homeostasis and cellular health of bivalves
116 when exposed to potentially toxicological compounds (Moore, 2004; Picot *et al.*, 2019).
117 Harmful algae-derived phycotoxins have recently been demonstrated to trigger autophagic
118 processes in different species of marine invertebrates, but particularly in *P. maximus*
119 contaminated with DA (García-Corona *et al.*, 2022; 2024).

120 The long retention of exogenous compounds also occurs through macroautophagy, a cellular
121 process analogous to autophagy where mammalian skin macrophages can incorporate and
122 retain tattoo ink into their cytoplasm. These ink-laden macrophages can exhibit lifespans as
123 long as the entire life of the tattooed animal, which explains the long-term tattoo persistence
124 and the difficulties to remove tattoos in mammalian skin cells (Flannagan *et al.*, 2012;
125 Gordon, 2016; Baranska *et al.*, 2018). Hence, we hypothesized that autophagy could be a kind
126 of analogous DA-tattooing mechanism in the digestive glands of *P. maximus*, and one reason
127 explaining the long retention of remaining DA in this species (García-Corona *et al.*, 2022).
128 Notwithstanding, to confirm that autophagy is involved in DA long-term retention, it would
129 be necessary to follow the succession of events that lead to autophagy during the
130 contamination and decontamination process. In this study, the localization of DA within
131 tissues of *P. maximus* during the contamination and decontamination phases, as well as its
132 toxicokinetics and the implication of autophagy was followed thanks to an
133 immunohistochemical time-tracking at the subcellular level, this in order to unveil for how
134 long DA is trapped within these autophagosomic structures.

135 **2. Materials and methods**

136 **2.1. Source of scallops and *P. australis* environmental data**

137 A total of 66 scallops *P. maximus* (5.1 ± 0.3 cm shell length, 42.8 ± 8.2 g total weight) were
138 reared in the field within culture-suspended cages at the Lanvéoc cove ($48^{\circ}29'56.3''$ N,
139 $4^{\circ}46'29.6''$ W; Bay of Brest, France) between February and October 2021. The information
140 on the cellular densities of all phytoplankton species, including the DA-producing *Pseudo-*
141 *nitzschia australis* in the area along the rearing period was obtained from the online database
142 REPHY (REseau d'observation et de surveillance du PHYtoplancton et de l'hydrologie dans
143 les eaux littorales, <https://bulletinrephytox.fr/accueil>) at the Lanvéoc cove. On March 30,
144 2021, a bloom of *P. australis* was recorded with densities reaching up to 6×10^4 cells L^{-1} and

145 lasted for ~15 days. To study the contamination process, sequential sampling of 11 scallops
146 per time point were carried out before the bloom of the toxic *P. australis* mentioned above on
147 February 22, 2021 and March 17, 2021 (corresponding to days 0 and 23 of the sampling,
148 respectively), during the bloom, on March 30, 2021, and April 07, 2021 (corresponding to
149 days 36 and 44 of the sampling, respectively), and after the bloom, on June 26, 2021, and
150 October 14, 2021 (corresponding to days 80 and 234 of the sampling, respectively).

151 To study the decontamination process, 60 wild scallops (9.7 ± 0.1 cm shell length, 168 ± 6.6
152 g total weight) were collected by dredging a natural bed in Camaret-sur-Mer, France ($48^{\circ} 26'$
153 $33.1''$ N, $4^{\circ} 35' 49.6''$ W) in early April 2021, eight days after the same bloom of *P. australis*
154 mentioned above ($\sim 6 \times 10^4$ cells L⁻¹, REseau d'observation et de surveillance du
155 PHYtoplancton et de l'hydrologie dans les eaux littorales, <https://bulletinrephytox.fr/accueil>)
156 to follow depuration of DA at laboratory.

157 **2.2. Depuration of DA in the laboratory and scallop dissection**

158 Scallops naturally contaminated with DA were transported to the Tinduff hatchery
159 (Plougastel-Daoulas, France) within a few hours after collection. Upon arrival at the
160 aquaculture facilities, the organisms were washed and scrubbed of epibionts, and immediately
161 distributed in two 800 L fiberglass tanks (30 scallops. tank⁻¹) with a sandy bottom. Filtered
162 seawater (1 μ m, activated carbon) was supplied and renewed in the tanks at 0.2 L min⁻¹
163 (complete renewal in 24 hours to minimize re-ingestion of feces) through a continuous
164 upstream-flow system with water pumped from the Bay of Brest. Animals were fed daily with
165 a diet consisting of 10×10^9 cells.scallop⁻¹day⁻¹ of the flagellate *Tisochrysis lutea*. These food
166 intakes were provided continuously by mixing the phytoplankton with the filtered water
167 supply. Each tank was covered with a canvas and illuminated separately by a LED spotlight
168 bar (NICREW Classic LED Plus 120-150 cm, 1150 lm) placed 1 m above the water surface
169 with a photoperiod set at 12h:12h (light: darkness). During the experiment, the water was
170 maintained fully oxygenated (100% O₂ saturated) and at a constant temperature of 15.9 °C,
171 and salinity of the pumped seawater within the Bay (*i.e.* between 32.5 and 34 PSU over the 2
172 months of the experiment). The scallops were maintained under these experimental conditions
173 for 60 days, with sequential sampling of 10 animals after 0, 7, 14, 21, 30, and 60 days of
174 depuration in the laboratory.

175 All sampled scallops were placed on a frozen plate to avoid suffering during sacrifice. The
176 flesh was carefully excised from the shells, and since the digestive gland (DG) accumulates \geq

177 80% of the total DA burdens (Blanco *et al.*, 2002a) this organ was carefully dissected and
178 separated from the rest of the tissues (RT = adductor muscle, gills, mantle, kidney, and gonad)
179 to avoid contamination of the other organs by DA of the DG during dissections (García-
180 Corona *et al.*, 2022). The DG of each animal was longitudinally sliced into two halves, one
181 stored at -20 °C to determine the toxin concentration in each individual, and the other fixed in
182 Davidson solution (Kim *et al.*, 2006) for anti-DA immunohistochemical purposes. The rest of
183 the tissues were only stored in Davidson solution for anti-DA immunohistochemical purposes.

184 **2.3. Domoic acid extraction and analysis**

185 Toxin was extracted exclusively from frozen DG of each scallop following the procedure
186 described by Quilliam *et al.* (1989) with modifications. Approximately 200 mg of tissue
187 homogenate was placed in a 2-mL Eppendorf tube containing 250 mg of glass beads (100–
188 250 µm diameter). Subsequently, 450 µL of MeOH:H₂O (1:1, v/v) was added. The sample
189 was ground using a Laboratory Mixer Mill MM 400 system (Retsch® Fisher Scientific,
190 Illkirch-Graffenstaden, FR) for 3 min at 30 Hz then centrifuged for 5 min at 15,000 g. The
191 supernatant was then transferred to a 1 mL volumetric flask. This operation was repeated,
192 then the two supernatants were combined in the flask, and the volume was adjusted to 1 mL
193 with MeOH:H₂O (1:1, v/v). Then, 800 µL of the crude extract were filtered through 1 mL 0.2
194 µm nylon centrifugal filters (VWR International, Radnor, PA, USA) at 10,000 g for 5 min at 4
195 °C, and aliquots of 200-µL the filtered extract were stored at -20 °C until analysis.

196 DA quantification was performed by HPLC-UV according to García-Corona *et al.* (2022)
197 with modification, using an Agilent (Santa Clara, CA, USA) 1260 Infinity LC system (pump,
198 refrigerated autosampler, column oven, diode array detector). Chromatographic separation
199 was carried out on a reversed-phase column Uptisphere TP C₁₈ (250 × 4.6 mm, 5 µm, 300 Å,
200 Interchim, Montluçon, France) with an isocratic mobile phase consisting of H₂O + CH₃CN
201 (9:1 v/v) with 0.1% of CF₃CO₂H. The flow rate was 1 mL.min⁻¹ and the column temperature
202 was maintained at 40 °C. The wavelength was set at 242 nm. The injection volume was 20
203 µL. The quantification was performed relative to the DA standard (National Research Council
204 Canada, NRCC) with a 5-point calibration curve over the concentration range 0.5 to 10.3
205 µg.mL⁻¹. The Limit of Quantification (LOQ) and the Limit of Detection (LOD) of the method
206 were 0.04 and 0.1 µg.m⁻¹, respectively, which corresponded to 0.2 and 0.5 mg DA.kg⁻¹ tissue,
207 respectively.

208 **2.4. Quantitative anti-DA immunohistochemistry**

209 In order to follow the *in situ* localization of the toxin at the subcellular level in the tissues
210 (digestive gland, gills, mantle, adductor muscle, kidney, and gonad) of the scallops in both
211 contamination and decontamination scenarios, a specific anti-DA immunohistochemical
212 protocol recently developed by García-Corona *et al.* (2022) was applied in this work with
213 minor modifications. Paraffin tissue sections (4- μm thickness) were rehydrated and incubated
214 overnight with a dilution (0.01 mg. mL^{-1}) of a Goat polyclonal anti-DA primary antibody
215 (Eurofins Abraxis[®], Warminster, PA, USA) at 4°C. The next day, the slides were incubated at
216 37 °C for 2 h with a dilution (0.001 mg. mL^{-1}) of an HRP sharped IgG Rabbit anti-Goat
217 secondary antibody (abcam[®], Cambridge, UK). Finally, samples were revealed with
218 diaminobenzidine (DAB+ Chromogen Substrate Kit, abcam[®], Cambridge, UK) for 1 h in
219 darkness at room temperature.

220 The qualitative description of DA localization in the digestive gland was made considering
221 the development stages of the digestive diverticula of the DG of *P. maximus* according to
222 Mathers (1976) (Fig. 1) as: (A) digestive diverticulum in a holding condition (Hd); cubical
223 digestive cells (dc) with few vacuoles (v) lining a large lumen (l) with secretory cells (sc)
224 easily identified. (B) diverticulum in absorptive condition (Ad); where few vacuoles (v) are
225 present in the apical region of the digestive cells (dc). (C) diverticulum in digestive condition
226 (Dd); where large digestive cells (dc) constitute the tubular region (tr) of the diverticula. (D)
227 diverticulum in advanced digestive condition (ADd); secretory cells (sc) are absent, the
228 digestive cells (dc) constitute the tubular region (tr) while the adipocyte-like cells (al)
229 compose the ascinar region (ar) of the diverticula. (E) diverticulum undergoing breakdown
230 (Bd); digestive cells (dc) show loss of structure and form in the ascinar region (ar) with
231 abundant adipocyte-like cells (al). (F) diverticulum showing regeneration (Rd); the secretory
232 cells (sc) are again visible at the junctions between the old (ascinar region) and new (tubular
233 region) diverticulum.

234 Three regions from each histological section of the digestive glands treated with the anti-DA
235 immunohistochemical protocol were randomly digitized at high resolution (63 \times
236 magnification; 600 dpi) using a Nikon D7500 DSLR camera connected to a Zeiss Axio
237 Observer Z1 light microscope (St Louis, MO, USA). The recorded images were processed
238 using the image analysis software Image Pro Plus, v. 4.5 (Media Cybernetics, Bethesda, MD).
239 In García-Corona *et al.* (2022), DA was mainly localized in structures identified as
240 autophagosomes and residual bodies in the cytoplasm of digestive cells. Therefore, a total of
241 378 micrographs (i.e. 3 micrographs from the DG of each scallop) were used to count the

242 number of total and positive DA-immunostained autophagosomes, as well as the number of
243 total and anti-DA stained residual bodies present in a predetermined area of $\sim 1.33 \text{ mm}^2$
244 (García-Corona *et al.*, 2024). Then, calculations of the occurrence of early and late DA-
245 autophagy in the DG of each scallop through contamination and depuration processes were
246 performed according to the following formulas, respectively:

$$DA \text{ early autophagy (\%)} = \frac{\text{anti - DA stained autophagosomes}}{\text{total number of autophagosomes}} \times 100$$

$$DA \text{ late autophagy (\%)} = \frac{\text{anti - DA stained residual bodies}}{\text{total number of residual bodies}} \times 100$$

247

248 **2.5. Statistical analysis**

249 Separate one-way analyses of variance (ANOVA, type II Sum of Squares) were applied to
250 determine statistically significant differences in toxin concentrations in the tissues, as well as
251 in the frequencies of early and late autophagy of DA in the DG of the scallops. *A priori*
252 Anderson-Darling and Fligner-killeen tests were applied to confirm the normality of
253 frequencies and homogeneity of variances of the residuals of the data, respectively (Hector,
254 2015). When needed, data were transformed (\log , $1/\chi$, or $\sqrt{\chi}$) prior to analysis to meet *a priori*
255 assumptions. The percentage-expressed values were also arcsine ($\arcsin \sqrt{P}$) transformed
256 (Zar, 2010), but all data are reported untransformed as the mean \pm standard error (SE) except
257 when indicated. As needed, *post hoc* comparisons of means with Tukey's honest significance
258 test (HSD) were performed to identify differences between means (Hector, 2015; Zar, 2010).
259 Pearson's correlation coefficients were run to assess the relationship between DA burdens and
260 the formation of autophagosomes and residual bodies in the DG of the animals during
261 contamination and decontamination process (Zar, 2010). Since the presence of toxic *P.*
262 *australis* was continuously observed throughout the field monitoring, DA depuration rate was
263 assessed only in the DG of experimental scallops maintained in the laboratory over the entire
264 2-month decontamination period. Depuration rate was calculated according to Dusek Jennings
265 *et al.* (2020) using the one-compartment exponential decay model, $DA_t = DA_0 \cdot e^{-rt}$, where
266 DA_t is the DA concentration after t days, DA_0 represents DA concentration at the end of the
267 depuration, t is days elapsed, and the slope of the equation (r) is the daily depuration rate.
268 DA_0 and the slope were estimated using linear regression after \ln -transformation of DA
269 burdens (Álvarez *et al.*, 2020), but untransformed data are presented. All data were analyzed

270 with a level of statistical significance set at $\alpha = 0.05$ using command lines in the R language
271 (R v. 4.2.2, R Core Team, 2020).

272 **3. Results**

273 **3.1. Toxin accumulation and depuration**

274 Changes in DA concentrations in the DG of scallops through the natural contamination
275 process are shown in Fig. 2A. The significantly lower toxin burdens in this organ were
276 recorded at the beginning of our monitoring (day 0), with 11.3 ± 1.3 mg DA. kg^{-1} ; this value
277 slightly increased (51.2 ± 3.9 mg DA. kg^{-1} , $P < 0.05$) after 23 days of monitoring and
278 following an exposure to a concentration of 800 cells L^{-1} of the toxic *P. australis*.
279 Nonetheless, the contamination rate of scallops peaked abruptly and significantly between 36
280 and 44 days after our first sampling during a *P. australis* bloom (6×10^4 and 2.1×10^4 cells L^{-1} ,
281 respectively recorded from March 30 to April 07, 2021) with average burdens of ~ 700 mg
282 DA. kg^{-1} in the DG of the scallops. Moreover, the highest interindividual variability in DA
283 accumulation was also observed through this period as evidenced by the high coefficients of
284 variation (CV, 31.8-28.6 %), and with values ranging from 86.5 up to 1,806.8 mg DA. kg^{-1} .
285 Although *P. australis* populations drastically decreased until disappearing after 80 days,
286 scallops remained strongly contaminated (290.2 ± 83.5 mg DA. kg^{-1}). At the last sampling
287 point, 234 days after the first sampling, *i.e.* 198 days after the first bloom, the concentrations
288 of DA in the DG of the animals were close to 32.3 ± 4.5 mg DA. kg^{-1} , Fig. 2A.

289 The depuration experiment in the laboratory started with heavily contaminated scallops, with
290 concentrations at ~ 2000 mg DA. kg^{-1} in the DG. Toxin burdens however did not significantly
291 decrease throughout the following 30 days. Even with a slight reduction ($P < 0.05$) of toxin
292 amounts in the DG between 30 and 60 days, the scallops were still highly contaminated
293 (1182.5 ± 105.9 mg DA. kg^{-1}) (Fig 2B). As seen in Fig. 2B, DA depuration rate in the DG of
294 the scallops was estimated at 0.001 day^{-1} from a one-compartment exponential decay model
295 that explained 52% of the variance, with a good statistical fit ($P < 0.05$) and without evidence
296 of over-dispersion of the data.

297 **3.2. Domoic acid *in situ* localization in a contamination and decontamination scenario**

298 The presence of DA was readily detected in the DG of scallops through a natural
299 contamination process (Fig. 2A and Fig. 3). As observed in Fig. 3A, the DA-chromogenic
300 signal appeared since day 0 of the field monitoring trapped within few early autophagosomes

301 (ea) of small size (~1-2.5 μm) distributed in the apical region of the cytoplasm of the
302 digestive cells (dc), particularly in the digestive diverticula (dd) in absorptive (Ad) condition.
303 Bigger residual bodies (rb) of ~5-10 μm and present only in the adipocyte-like cells (al) in the
304 ascinar region (ar) of the digestive diverticula undergoing breakdown (Bd) acquired a slight
305 anti-DA staining. During the period of steady contamination (days 23 to 80, Fig. 3B-E), an
306 intense process of early autophagy of the toxin was observed. The appearance of numerous
307 early autophagosomes (ea) with a positive anti-DA signal was detected mainly in the apical
308 zone of the digestive cells in the tubular region (tr) within the digestive diverticula in active
309 (Dd) and advanced (ADd) digestion, as well as the digestive diverticula undergoing
310 breakdown (Bd) or showing regeneration (Rd). The formation of late autophagosomes (la) of
311 bigger size (~ 3-5 μm) than early autophagosomes with positive DA-labeling and present in
312 the basal zone of digestive cells was also detected mainly in digestive diverticula in stages of
313 active or advanced digestion, or in the diverticula showing regeneration. Through this period,
314 the presence of some residual bodies with DA-chromogenic signal also occurred in the
315 digestive diverticula undergoing breakdown or regeneration. Finally, at the end of the
316 contamination surveillance (day 234, Fig. 3F), a low prevalence of early autophagosomes was
317 observed in the digestive diverticula in absorption condition, while a high number of residual
318 bodies with an intense anti-DA signal were found widely distributed in the DG of scallops.

319 On the other hand, in the laboratory DA-depuration scenario, a strong process of early (ea)
320 and late autophagy (la) of the toxin was already activated in highly contaminated scallops
321 since day 0, mainly in digestive diverticula in advanced digestion (ADd), with only few-dyed
322 residual bodies (rb) in the DG (Fig. 4A). As shown in Figs. 4B-C, over the following 7 to 14
323 days of DA-depuration, a similar amount (40-50 %) of early and late autophagy of the toxin
324 was observed in the DG of the animals, with the presence of autophagosomes and residual
325 bodies with chromogenic signal mostly in the digestive diverticula showing regeneration
326 (Rd). Notwithstanding, between days 21 and 30 of scallop conditioning, the early autophagy
327 of the toxin was negligible, and it was observed how the labeled late autophagosomes
328 gathered in the digestive diverticula undergoing breakdown to give rise to residual bodies
329 with intense anti-DA signal, that were distributed throughout the DG (Fig. 4D-E). At the end
330 of the toxin depuration period (day 60, Fig. 4F), almost no DA autophagy was observed in the
331 digestive diverticula in absorption stages either, with a high prevalence and intensity of DA-
332 labeling in the residual bodies widely distributed in the DG.

333 The quantitative IHC analyses allowed to corroborate the overall microanatomical
334 observations described above (Fig. 5). Across natural contamination of scallops during ASP
335 bloom, early DA-autophagy (autophagosomes with DA-chromogenic signal) in the DG
336 increased steadily and significantly from day 0 ($36.6 \pm 7.6 \%$) to its highest values on day 44
337 ($74 \pm 3 \%$), then, these frequencies decreased to its lowest values ($P < 0.05$) at the end of the
338 surveillance ($25.9 \pm 3.2 \%$) after 234 days (Fig. 5A). Whereas late DA-autophagy frequencies
339 (Fig. 5A) showed slight increases ($P < 0.05$) of stained-residual bodies between 0 days ($3.6 \pm$
340 2%) and 44-80 days ($28.9 \pm 6 \%$, and $19.5 \pm 4.6 \%$, respectively). However, the amount of
341 stained residual bodies significantly peaked up to its highest frequency ($92.8 \pm 1.5 \%$) at the
342 end of the field monitoring. Under this scenario, early DA-autophagy was strongly and
343 directly correlated ($r = 0.8$, $P < 0.05$) with DA accumulation in the DG, while the relationship
344 between the proliferation of anti-DA autophagosomes and residual bodies was negative and
345 significant but not strong ($r = -0.46$). The correlation between toxin burdens and DA-stained
346 residual bodies in the DG was low ($r = -0.21$) and non-significant.

347 Conversely, as shown in Fig. 5B, an inverse pattern between early and late autophagy was
348 found along DA-depuration process ($r = -0.8$, $P < 0.05$). The frequencies of IHC-labeled
349 autophagosomes decreased ($P < 0.05$) from $76.2 \pm 2.6 \%$ at the beginning of the experiment, to
350 $\sim 49.7 \%$ between days 7 and 14, to then continue dropping to the minimum values ($P < 0.05$)
351 of $\sim 11.5 \%$ at the end of the experiment. While the amount of residual bodies significantly
352 raised from the start ($21.9 \pm 3.7 \%$) to days 7 and 14 ($\sim 44.5 \%$) and subsequently peaked at
353 its highest frequencies ($\sim 88.1 \%$, $P < 0.05$) at the end of the laboratory depuration.
354 Furthermore, a negative and significant relationship ($r = -0.5$) was found between DA
355 amounts and late autophagy (anti-DA residual bodies) in the DG of the scallops.

356 Through the application of the specific IHC technique it was possible to detect a positive anti-
357 DA chromogenic dye in some other tissues of highly contaminated scallops during both
358 contamination and decontamination processes (Fig. 6). Toxin labeling was observed mainly in
359 the microvilli of the branchial filaments (Fig. 6A), as well as in the axons and the somal body
360 of the neurons embedded between the bundles of the adductor muscle (Fig. 6B). Moreover,
361 anti-DA hues were also localized in the globose cells of the gonad ducts embedded in the
362 male and female parts of the gonads of the scallops (Fig. 6C and D, respectively). Finally, no
363 brown anti-DA signal was observed in the mantle or kidney of the scallops.

364 4. Discussion

365 A clear gap exists in knowledge about the physiological causes of the long retention of DA in
366 king scallops *P. maximus*. The understanding of the biological mechanisms involved in both
367 DA accumulation and depuration processes is of the utmost importance since the toxicity of
368 scallop stocks during and after *Pseudo-nitzschia* blooms, and the kinetics of contamination
369 and depuration of DA determines the consequent exploitation capacity of this resource. The
370 ability to accumulate, retain, and redistribute DA burdens between different organs differs
371 greatly between bivalve species (Blanco *et al.*, 2002b; Basti *et al.*, 2018). Furthermore, there
372 is vast evidence that, in bivalves, DA depuration time is species-specific and has a wide range
373 of variability. Most fast DA-depurators like mussels (Wohlgeschaffen *et al.* 1992; Novaczek
374 *et al.*, 1992; Blanco *et al.* 2002b; Mafra *et al.*, 2010), many clams (Gilgan *et al.* 1990; Dusek
375 Jennings *et al.*, 2020; Álvarez *et al.*, 2015; Blanco *et al.*, 2010), some oysters (Jones *et al.*,
376 1995; Mafra *et al.*, 2010), and even scallops (Álvarez *et al.*, 2020) are capable of detoxifying
377 DA burdens up to 900 mg. kg⁻¹ within hours or a few days, with detoxification rates ranging
378 from 0.1 to ~ 2 day⁻¹ in the whole body, and up to 10 day⁻¹ in digestive tissues. Hence,
379 retaining DA for a short time with a low impact on their harvest and commercialization.

380 Nonetheless, *P. maximus* is a particular case, since, as found in this work, the DA depuration
381 rate calculated for the scallops in the digestive gland in this work was very low (0.001 day⁻¹)
382 when compared to those of the bivalves mentioned above, but similar to that reported for the
383 same species in the same organ by Blanco *et al.* (2002a, 2006) of about 0.003 and 0.007 day⁻¹,
384 respectively. Notwithstanding, these depuration rates are too low even against those found in
385 the digestive gland of other bivalves classified as slow DA-depurators as well, like *P.*
386 *magellanicus* (~ 0.2 day⁻¹, Wohlgeschaffen *et al.*, 1992; Douglas *et al.*, 1997) and *S. patula*
387 (0.05 and 0.02 day⁻¹, Horner *et al.*, 1993; Dusek Jennings *et al.*, 2020, respectively). Thus,
388 demonstrating that *P. maximus* has the slowest DA-depuration kinetics among bivalves
389 studied until now. In fact, using the depuration rate estimated in this study, it would take more
390 than one year for the scallops of our experiment to almost depurate the total burdens of DA in
391 the digestive gland. This duration is calculated under an environment virtually free of toxic
392 *Pseudo-nitzschia*, which is practically impossible with the continuous presence of *P. australis*
393 in the natural environment, as observed through the field monitoring in this work, and the
394 repeated seasonal blooms of this species registered several times a year on the northwest coast
395 of France (Amzil *et al.*, 2001; Husson *et al.*, 2016; Ayache *et al.*, 2019; REPHY-ifremer).

396 In this work, the DA contents measured in field-based scallops were the result of the
397 continuously accumulated and subsequently depurated toxin. Therefore, differences in DA

398 accumulation-depuration in the organisms were strongly dependent on the toxicity of the
399 *Pseudo-nitzschia* cells, the duration of the ASP blooms, the time through the animals were
400 exposed to toxic microalgae and the moment at which the organisms were sampled during the
401 bloom. This has a strong repercussion on the precision of the measurements of DA
402 depuration rates in natural stocks. Therefore, it has to be taken into account during ASP-
403 monitoring programs, either to avoid unnecessary fishery closures or to ensure public safety.
404 To date, the only alternative for the profession to accelerate DA depuration of king scallops
405 would be keeping contaminated animals in water systems free of toxic *Pseudo-nitzschia*
406 during several months such as those used in this work for DA depuration, or the evisceration
407 of the inedible and highly contaminated tissues (i.e. digestive gland) to reduce the toxin
408 content of the product. Nevertheless, these solutions would not be economically feasible
409 considering the space required for the conditioning of scallops, and the cost of such a
410 procedures (F. Breton, *pers com*, 2023; Vanmaldergem *et al.*, 2023).

411 Moreover, there is a high inter-individual variability in the toxin burdens in the scallops.
412 These large variations in DA contents, particularly in the DG (CV ranging from 30 to 125%)
413 seem to be a characteristic of this species, as it was detected in several other studies (Blanco
414 *et al.*, 2002a, 2006; Bogan *et al.*, 2007; García-Corona *et al.*, 2022). Nonetheless, the actual
415 physiological reasons for these profound differences in DA accumulation/depuration rates
416 between bivalves are still unclear. Recently, Alvarez *et al.* (2020) designed a multi-
417 compartment model that suggests DA accumulated by *A. pupuratus* is rapidly transferred
418 from the digestive gland to other organs such as the gonad, muscle, mantle, gills, but
419 particularly the kidney, which depurate the toxin independently and with much more
420 efficiency following a first-order exponential decay. The same strategy was proposed to
421 explain the rapid detoxification of visceral DA in *Mytilus edulis* and *Crassostrea virginica*
422 (Mafra *et al.*, 2010), as well as in *Mesodesma donacium* (Álvarez *et al.*, 2015) during early
423 toxin uptake phase. Nonetheless, there is evidence that in the king scallop, DA redistribution
424 from the digestive gland to other tissues, including the kidney, does not seem to occur, since
425 previous findings demonstrate that the small fraction ($\leq 5\%$) of total DA stored in the rest of
426 the tissues is excreted at a rate 2.5-fold faster than in the digestive gland (Blanco *et al.*, 2002a,
427 2006). Throughout our monitoring of contamination and decontamination of the scallops, DA-
428 staining in the rest of the tissues (gonad, muscle, gills, and gonads) was only observed in
429 specific structures of the most contaminated scallops ($\sim 800\text{-}2000 \text{ mg DA kg}^{-1}$) in the entire
430 study. The DA-signal was visualized in the microvilli of the gills and the globose cells

431 embedded in the spawning ducts of the gonads. A similar result was reported by García-
432 Corona *et al.* (2022) in strongly DA-contaminated scallops *P. maximus*, where
433 immunoreactivity occurred in mucus-producing structures. So far, it has not been confirmed
434 whether DA has a simple chemical affinity to the mucus by some intermolecular forces, or if
435 it is chemically bound to any component of the mucus. Nevertheless, as discussed above,
436 since the amount of toxin in the rest of the tissues is negligible, it can be inferred that mucus
437 production does not play an important role in toxin depuration in this species. Interestingly,
438 DA IHC-staining was also found in the peripheral neural tissue of the scallops, particularly in
439 the axon extensions and the soma body of some neurons embedded in the adductor muscle.
440 The presence of high DA-affinity and low-sensitivity receptors has been identified in tissues
441 of other bivalve species like *S. patula* (Trainer and Bill, 2004), which could indicate the
442 presence of this type of receptors in *P. maximus*. Further studies are necessary to corroborate
443 all these ideas.

444 As the digestive gland appeared as the key organ for the storage and depuration of DA in *P.*
445 *maximus*, we focused on this organ to go deeper into the cause of the long retention of DA in
446 *P. maximus*. No depuration of DA accumulated in the digestive gland of scallops was
447 observed within the first 30 days of conditioning in the laboratory, with a slight reduction of
448 DA burdens in this organ after 60 days of depuration. Our results put in evidence that during
449 the period of active contamination, an intense process of early DA-autophagy was triggered,
450 with the formation of autophagosomes in the apical region of the digestive cells cytoplasm,
451 mainly within the digestive diverticula in absorptive and active digestion stages. According to
452 Owen (1972) and Mathers (1976), this suggests an early and active assimilation of recently
453 ingested food particles into the cells for digestion. Whereas the appearance of bigger
454 autophagosomes in the distal cytoplasmic zone of digestive cells, such as those observed in
455 the digestive diverticula in stages of advanced digestion, indicates the end of intracellular
456 digestion or the early formation of residual bodies (Mathers, 1976; Yurchenko and Kalachev,
457 2019). On the other hand, the high intensity and prevalence of residual bodies with strong
458 anti-DA signal widely distributed in digestive diverticula under breakdown or showing
459 regeneration until the end of the depuration process reveal that DA is not completely excreted
460 from the cells, remaining in the digestive gland for an indefinite time, as described in the
461 literature (Owen, 1972; Cuervo, 2004; McMillan, 2018). This work constitutes evidence of
462 the importance of autophagy in the toxicokinetics of DA in *P. maximus*. The long retention of
463 exogenous compounds does not appear to be a phenomenon exclusively related to autophagy;

464 it also occurs in other types of cells under analogous cellular processes. Through macrophagy,
465 specialized cells called macrophages use their cytoplasmic membranes to phagocytose large
466 extracellular particles ($\geq 0.5 \mu\text{m}$, e.g. bacteria and metabolic debris) via endocytosis, creating
467 internal vesicular compartments called phagosomes. Phagosomes with cargo materials fuse
468 with lysosomes, forming phagolysosomes, leading to enzymatic degradation (Flannagan *et*
469 *al.*, 2012; Gordon, 2016). There is evidence that, upon tattooing, mouse and human dermal
470 macrophages are capable of: 1) phagocytosing pigment particles through several capture-
471 release-recapture cycles across cell regeneration, or 2) exhibiting lifespans as long as the adult
472 life of tattooed animals, accounting for both long-term persistence and strenuous removal of
473 tattoo ink on the skin. Even when the macrophages laden with tattoo ink die and release the
474 pigments, the staining particles remain in the extracellular space at the site of tattooing where
475 they are recaptured by new macrophages (Baranska *et al.*, 2018). Like autophagy,
476 macrophagy is a catabolic mechanism used to remove pathogens and cellular waste for
477 detoxification or nutrient recycling purposes, in which macrophages can exhibit lifespans of
478 months to years (Flannagan *et al.*, 2012; Gordon, 2016; Baranska *et al.*, 2018).

479 The results of this work and the discussed above suggest two new hypotheses: 1) DA may
480 undergo successive cycles of capture–release–recapture by autophagosomic structures
481 through the regenerative cycle of digestive cells of the scallops, or 2) autophagosomes and
482 residual bodies with DA exhibit long lifespans without any toxin vanishing from months to
483 years, thus triggering an analogous long-term DA-tattooing in the digestive glands of *P.*
484 *maximus*. The direct and strong relationship found between early autophagy and DA
485 accumulation, as well as the formation of residual bodies with depuration of the toxin denote
486 that, at the subcellular level, autophagy could modulate the long-retention of DA in the
487 digestive cells of *P. maximus*, by trapping the toxin and making it inaccessible to the
488 detoxification system. The findings of this work are also reinforced by those of Ventoso *et al.*
489 (2021) since the intramuscular injection of DA in *P. maximus* led to the overexpression of
490 some genes related to autophagy and vesicle-mediated transport. Another question to be
491 answered is the fate of the residual bodies with DA labeling after regeneration of digestive
492 cells. Mathers (1976) demonstrated that the digestion cycle in the DG of *P. maximus* is
493 closely correlated with the feeding tidal rhythm, where the intracellular digestion process of
494 phagocytosed food materials is accomplished within a biphasic 12-h tidal cycle (24h total),
495 including the formation of autophagosomes in cells showing active digestion, to the
496 disintegration of residual bodies in the diverticula undergoing breakdown or showing

497 regeneration. The fact that DA is recognized by the anti-DA antibody despite several and
498 relatively short time frames of cellular digestion mentioned before indicates the toxin is not
499 being degraded. Therefore, the rapid cycles of cellular digestion are completely independent
500 of the digestion, breakdown, and subsequent excretion of DA. This strengthens the DA-
501 tattooing hypothesis proposed in this study, given the long persistence (up to several months)
502 of DA-labeled autophagosomes and residual bodies observed in the digestive diverticula of *P.*
503 *maximus* through the entire process of contamination and depuration of the toxin.

504 **Conclusions**

505 The *in situ* DA-immunodetection method applied in this work is a powerful tool to perform a
506 subcellular time-tracking of domoic acid in tissues of king scallops during contamination and
507 depuration phases. Early autophagy, with the formation of autophagosomes, appeared actively
508 involved in the accumulation of the toxin in the digestive gland. This study also provides a
509 strong presumption that the long retention of a portion of DA initially accumulated in king
510 scallops is due to late autophagy, with the occurrence and long persistence of DA-labeled
511 residual bodies, resembling an analogous DA-tattoo in the digestive gland of *P. maximus*. The
512 quantitative immunohistochemical information developed in this work could be valuable for
513 the development of numeric models that allow predicting the dynamics of contamination and
514 decontamination with DA in natural fishery stocks. Moreover, our findings represent a
515 cornerstone in the proposal of strategies to accelerate the depuration kinetics of ASP-toxin in
516 this species.

517 **Acknowledgments**

518 The authors are deeply grateful to Sylvain Enguehard (Novakits, Nantes) for providing the
519 non-commercial primary antibodies necessary to carry out this study, as well as Valentin
520 Siebert, Erwan Amice, and Julien Thebault (LEMAR, Brest) for help with scallop collection.
521 We also thank Margot Deeglise and Guillaume Bourhis, as well as all the Tinduff hatchery
522 staff for assistance with scallop rearing overall the entire depuration experiment. We thank
523 Marie Calvez, and Sébastien Artigaud (LEMAR, Brest) for assistance with tissue sectioning,
524 and antibodies quantification, respectively, as well as Carmen Rodríguez-Jaramillo and Raúl
525 Martínez-Rincón (CIBNOR, La Paz) for advices to optimize non-commercial antibodies for
526 the IHC analysis, and for help improving R-scripts, respectively. Special thanks to Guadalupe
527 Marrujo for sharing on her social media the article "Baranska *et al.*, 2018. Unveiling skin

528 macrophage dynamics explains both tattoo persistence and strenuous removal. *J Exp Med*"
529 that inspired the DA-tattoo hypothesis in *P. maximus* of this work.

530 **Declaration of competing interest**

531 The authors declare that they have no known competing financial interests or personal
532 relationships that could have appeared to influence the work reported in this paper.

533 **Funding**

534 This work received financial support from the research project "MaSCoET" (Maintien du
535 Stock de Coquillages en lien avec la problématique des Efflorescences Toxiques) financed by
536 France Filière Pêche and Brest Métropole, and from the project HIPPO financed by the
537 Agence Nationale de la Recherche (grant no. ANR-18-CE92-0036-01). JLGC was recipient of
538 a doctorate fellowship from CONACyT, Mexico (REF: 2019- 000025-01EXTF-00067), and
539 JVM was financed by Actiris International European Youth Mobility Program.

540 **Data availability statement**

541 The evidence and data that support the findings of this study are available from the
542 corresponding author upon reasonable request.

543 **Ethics statements**

544 The organisms used in this work were transported and handled according to the International
545 Standards for the Care and Use of Laboratory Animals. The number of sampled animals
546 contemplated "the rule of maximizing information published and minimizing unnecessary
547 studies". In this sense, 126 scallops were considered the minimum number of organisms
548 needed for this work.

549 **Author contributions**

550 Conceived the study: JLGC, HH, CF. Provided environmental data: AT, Performed the
551 experiments: HH, JV, FB. Sampling: JLGC, JV, FB, CF, HH. Processed the samples: JLGC,
552 JV, AD, SP, LB. Analyzed the data: JLGC, AD. Interpretation of data: JLGC, CF, HH.
553 Contributed reagents/materials/analysis tools: CF, HH, AD, SP, FB. Wrote the first draft of
554 the manuscript: JLGC. Writing – review & editing: CF, HH, JLGC.

555 **Literature cited**

- 556 Álvarez, G., Rengel, J., Araya, M., Álvarez, F., Pino, R., Uribe, E., Díaz, P.A., Rossignoli,
557 A.E., López-Rivera, A., Blanco, J., 2020. Rapid domoic acid depuration in the scallop
558 *Argopecten purpuratus* and its transfer from the digestive gland to other organs. *Toxins*,
559 12, 698. <https://doi.org/10.3390/toxins12110698>.
- 560 Álvarez, G., Uribe, E., Regueiro, J., Martin, H., Gajardo, T., Jara, L., Blanco, J., 2015.
561 Depuration and anatomical distribution of domoic acid in the surf clam *Mesodesma*
562 *donacium*. *Toxicon*, 102, 1–7. <https://doi.org/10.1016/j.toxicon.2015.05.011>.
- 563 Amzil, Z., Fresnel, J., Le Gal, D., Billard, C., 2001. Domoic acid accumulation in French
564 shellfish in relation to toxic species of *Pseudo-nitzschia multiseriata* and *P.*
565 *pseudodelicatissima*. *Toxicon*, 39(8), 1245–1251. [https://doi.org/10.1016/S0041-](https://doi.org/10.1016/S0041-0101(01)00096-4)
566 [0101\(01\)00096-4](https://doi.org/10.1016/S0041-0101(01)00096-4).
- 567 Ayache, N., Hervé, F., Lundholm, N., Amzil, Z., & Caruana, A. M. N., 2019. Acclimation of
568 the Marine Diatom *Pseudo-nitzschia australis* to Different Salinity Conditions: Effects on
569 Growth, Photosynthetic Activity, and Domoic Acid Content. In T. Mock (Ed.), *Journal of*
570 *Phycology* (Vol. 56, Issue 1, pp. 97–109). Wiley. <https://doi.org/10.1111/jpy.12929>.
- 571 Baranska, A., Shawket, A., Jouve, M., Baratin, M., Malosse, C., Voluzan, O., Vu Manh, T.-
572 P., Fiore, F., Bajénoff, M., Benaroch, P., Dalod, M., Malissen, M., Henri, S., Malissen, B.,
573 2018. Unveiling skin macrophage dynamics explains both tattoo persistence and strenuous
574 removal. *Journal of Experimental Medicine*, 215(4), 1115–1133.
575 <https://doi.org/10.1084/jem.20171608>.
- 576 Basti, L., Hégarret, H., Shumway, S.E. 2018. Harmful Algal Blooms and Shellfish. In:
577 Harmful Algal Blooms: A Compendium Desk Reference, First Edition. Shumway, S.E.,
578 Burkholder, J.M., Morton, S.L. (eds). John Wiley & Sons Ltd.
- 579 Bates, S.S., Hubbard, K.A., Lundholm, N., Montresor, M., Leaw, C.P. 2018. *Pseudo-*
580 *nitzschia*, *Nitzschia*, and domoic acid: new research since 2011. *Harmful Algae*, 79, 3-43.
581 <https://doi.org/10.1016/j.hal.2018.06.001>.
- 582 Blanco, J., Acosta, C., Bermúdez de la Puente, M., Salgado, C., 2002a. Depuration and
583 anatomical distribution of the amnesic shellfish poisoning (ASP) toxin domoic acid in the
584 king scallop *Pecten maximus*. *Aquatic Toxicology*, 60 (1-2), 111–121.
585 [https://doi.org/10.1016/S0166-445X\(01\)00274-0](https://doi.org/10.1016/S0166-445X(01)00274-0).
- 586 Blanco, J., Acosta, C.P., Mariño, C., Muñiz, S., Martín, H., Moroño, A., Correa, J., Arévalo,
587 F., Salgado, C., 2006. Depuration of domoic acid from different body compartments of the
588 king scallop *Pecten maximus* grown in raft culture and natural bed. *Aquatic Living*
589 *Resources*, 19 (3), 257–265. <https://doi.org/10.1051/alr:2006026>.
- 590 Blanco, J., Bermúdez, M., Arévalo, F., Salgado, C., Moroño, A., 2002b. Depuration of
591 mussels (*Mytilus galloprovincialis*) contaminated with domoic acid. *Aquatic Living*
592 *Resources*, 15, 53–60. [https://doi.org/10.1016/S0990-7440\(01\)01139-1](https://doi.org/10.1016/S0990-7440(01)01139-1).

- 593 Blanco, J., Livramento, F., Rangel, I. M., 2010. Amnesic shellfish poisoning (ASP) toxins in
594 plankton and molluscs from Luanda Bay, Angola. *Toxicon*, 55(2–3), 541–546.
595 <https://doi.org/10.1016/j.toxicon.2009.10.008>.
- 596 Blanco, J., Mauríz, A., Álvarez, G., 2020. Distribution of Domoic Acid in the Digestive
597 Gland of the King Scallop *Pecten maximus*. *Toxins*, 12(6), 371.
598 <https://doi.org/10.3390/toxins12060371>.
- 599 Bogan, Y. M., Kennedy, D. J., Harkin, A. L., Gillespie, J., Vause, B. J., Beukers-Stewart, B.
600 D., Hess, P., Slater, J.W., 2007. Variation in domoic acid concentration in king scallop
601 (*Pecten maximus*) from fishing grounds around the Isle of Man. *Harmful Algae*, 6, 81–92.
602 <https://doi.org/10.1016/j.hal.2006.07.002>.
- 603 Bresnan, E., Fryer, R. J., Fraser, S., Smith, N., Stobo, L., Brown, N., & Turrell, E., 2017. The
604 relationship between *Pseudo-nitzschia* (Peragallo) and domoic acid in Scottish shellfish.
605 *Harmful Algae*, 63: 193–202. <https://doi.org/10.1016/j.hal.2017.01.004>.
- 606 Cuervo, A.M., 2004. Autophagy: many paths to the same end. *Molecular and Cellular*
607 *Biochemistry*, 263 (1/2), 55–72. <https://doi.org/10.1023/b:mcbi.0000041848.57020.57>.
- 608 Douglas, D.J., Kenchington, E.R., Bird, C.J., Pocklington, R., Bradford, B., Silvert, W. 1997.
609 Accumulation of domoic acid by the sea scallop (*Placopecten magellanicus*) fed cultured
610 cells of toxic *Pseudo-nitzschia multiseriata*. *Canadian Journal of Fisheries and Aquatic*
611 *Sciences*, 54 (4), 907–913. <https://doi.org/10.1139/f96-333>.
- 612 Drum, A.S., Siebens, T.L., Crecelius, E.A., Elston, R.A. 1993. Domoic acid in the Pacific
613 razor clam *Siliqua patula* (Dixon, 1789). *Journal of Shellfish Research*, 12, 443–450.
- 614 Dusek Dusek Jennings, E., Parker, M. S., Simenstad, C. A., 2020. Domoic acid depuration by
615 intertidal bivalves fed on toxin-producing *Pseudo-nitzschia multiseriata*. *Toxicon*, 6,
616 100027. <https://doi.org/10.1016/j.toxcx.2020.100027>.
- 617 Flannagan, R. S., Jaumouillé, V., Grinstein, S., 2012. The Cell Biology of Phagocytosis.
618 *Annual Review of Pathology: Mechanisms of Disease*, 7(1), 61–98.
619 <https://doi.org/10.1146/annurev-pathol-011811-132445>.
- 620 García-Corona, J. L., Hégarret, H., Deléglise, M., Marzari, A., Rodríguez-Jaramillo, C.,
621 Foulon, V., Fabioux, C., 2022. First subcellular localization of the amnesic shellfish toxin,
622 domoic acid, in bivalve tissues: Deciphering the physiological mechanisms involved in its
623 long-retention in the king scallop *Pecten maximus*. *Harmful Algae*, 116.
624 <https://doi.org/10.1016/j.hal.2022.102251>.
- 625 García-Corona, J.L., Hegaret, H., Lassudrie-Duchesne, M., Derrien, A., Terre-Terrillon, A.,
626 Delaire, T., Fabioux, C. 2023. Comparative study of domoic acid accumulation, isomer
627 content and associated digestive subcellular processes in five marine invertebrate species.
628 *Aquatic toxicology*, 266, 106793. <https://doi.org/10.1016/j.aquatox.2023.106793>.

629 Gilgan, M.W., Burns B.G., Landry, G.J., 1990. Distribution and magnitude of domoic acid
630 contamination of shellfish in Atlantic Canada. In: E. Graneli, B. Sundstrom, L. Edler, D.M.
631 Anderson (Eds.), Toxic Marine Phytoplankton. Elsevier, N.Y. pp. 469- 474.

632 Gordon, S., 2016. Phagocytosis: An Immunobiologic Process. *Immunity*, 44(3), 463–475.
633 <https://doi.org/10.1016/j.immuni.2016.02.026>.

634 Hallegraeff, G. M. (1993). A review of harmful algal blooms and their apparent global
635 increase. In *Phycologia* (Vol. 32, Issue 2, pp. 79–99). Informa UK Limited.
636 <https://doi.org/10.2216/i0031-8884-32-2-79.1>.

637 Hector, A., 2015. The new statistics with R: an introduction for biologists, 1st ed. Oxford
638 University Press, New York.

639 Horner, R.A., Kusske, M.B., Moynihan, B.P., Skinner, R.N., Wekell, J.C., 1993. Retention of
640 Domoic Acid by Pacific Razor Clams, *Siliqua patula* (Dixon, 1789): Preliminary Study.
641 *Journal of Shellfish Research*, 12, 451–456.

642 Husson, B., Hernández-Fariñas, T., Le Gendre, R., Schapira, M., Chapelle, A., 2016. Two
643 decades of *Pseudo-nitzschia spp.* blooms and king scallop (*Pecten maximus*)
644 contamination by domoic acid along the French Atlantic and English Channel coasts:
645 Seasonal dynamics, spatial heterogeneity and interannual variability. *Harmful Algae*, 51,
646 26–39. <https://doi.org/10.1016/j.hal.2015.10.017>

647 Jones, T.O., Whyte, J.N.C., Ginther, N.G., Townsend, L.D., Iwama, G.K., 1995. Haemocyte
648 changes in the pacific oyster, *Crassostrea gigas*, caused by exposure to domoic acid in the
649 diatom *Pseudo-nitzschia pungens* f. multiseriis. *Toxicon*, 33 (3), 347–353.
650 [https://doi.org/10.1016/0041-0101\(94\)00170-](https://doi.org/10.1016/0041-0101(94)00170-)

651 Kim, Y., Ashton-Alcox, K.A., Powell, E.N., 2006. Histological Techniques for Marine
652 Bivalve Molluscs: update. NOAA Technical Memorandum NOS NCCOS 27, Maryland.

653 La Barre, S., Bates, S.S. Quilliam, M.A. 2014. Domoic acid. In. Outstanding marine
654 molecules: chemistry, biology, analysis. Edited by S. La Barre and J.-M. Kornprobst.
655 Wiley-VCH Verlag GmbH & Co. KgaA, Weinheim, Germany, pp. 189–216.

656 Lelong, A., Hégaret, H., Soudant, P., Bates, S.S. 2012. *Pseudo-nitzschia* (Bacillariophyceae)
657 species, domoic acid and amnesic shellfish poisoning: revisiting previous paradigms.
658 *Phycologia*, 51 (2), 168–216. <https://doi.org/10.2216/11-37.1>.

659 MacKenzie, J.D., Bavington, C, (2002). Measurement of Domoic Acid in King Scallops
660 processed in Scotland. Final Report for The Food Standards Agency Scotland.
661 https://www.foodstandards.gov.scot/downloads/Domoic_Acid_in_King_Scallops.pdf.

662 Mafra, L.L., Bricelj, V.M., Fennel, K., 2010. Domoic acid uptake and elimination kinetics in
663 oysters and mussels in relation to body size and anatomical distribution of toxin. *Aquatic*
664 *Toxicology*, 100 (1), 17–29. <https://doi.org/10.1016/j.aquatox.2010.07.0>.

665 Mathers, N.F., 1976. The effects of tidal currents on the rhythm of feeding and digestion in
666 *Pecten maximus* L. *Journal of Experimental Marine Biology and Ecology*, 24 (3), 271–
667 283. [https://doi.org/10.1016/0022-0981\(76\)90059-9](https://doi.org/10.1016/0022-0981(76)90059-9).

668 Mauríz, A., Blanco, J., 2010. Distribution and linkage of domoic acid (amnesic shellfish
669 poisoning toxins) in subcellular fractions of the digestive gland of the scallop *Pecten*
670 *maximus*. *Toxicon*, 55 (2-3), 606–611. <https://doi.org/10.1016/j.toxicon.2009.10>.

671 McMillan, D.B., Harris, R.J., 2018. The Animal Cell. In An Atlas of Comparative Vertebrate
672 Histology (pp. 3–25). Elsevier. <https://doi.org/10.1016/b978-0-12-410424-2.00001-9>.

673 Mizushima, N., Ohsumi, Y., & Yoshimori, T., 2002. Autophagosome Formation in
674 Mammalian Cells. *Cell Structure and Function*, 27(6): 421–429.
675 <https://doi.org/10.1247/csf.27.421>.

676 Moore, M.N., 2004. Diet restriction induced autophagy: a lysosomal protective system against
677 oxidative- and pollutant-stress and cell injury. *Marine Environmental Research*, 58 (2–5),
678 603–607. <https://doi.org/10.1016/j.marenvres.2004.03>.

679 Novaczek, I., Madhyastha, M.S., Ablett, R.F., Donald, A., Johnson, G., Nijjar, M.S., Sims,
680 D.E., 1992. Depuration of domoic acid from live blue mussels (*Mytilus edulis*). *Canadian*
681 *Journal of Fisheries and Aquatic Sciences*, 49 (2), 312–318. <https://doi.org/10.1139/f92-035>.

682

683 Owen, G., 1972. Lysosomes, peroxisomes and bivalves. *Science Progress* 60 (239), 299–318.

684 Picot, S., Morga, B., Faury, N., Chollet, B., Dégremont, L., Travers, M.A., Renault, T., Arzul,
685 I., 2019. A study of autophagy in hemocytes of the Pacific oyster *Crassostrea gigas*.
686 *Autophagy*, 1–9. <https://doi.org/10.1080/15548627.2019.1596>.

687 Pulido, O.M. 2008. Domoic Acid Toxicologic Pathology: A Review. *Marine Drugs*, 6, 180-
688 219. <https://doi.org/10.3390/md20080010>.

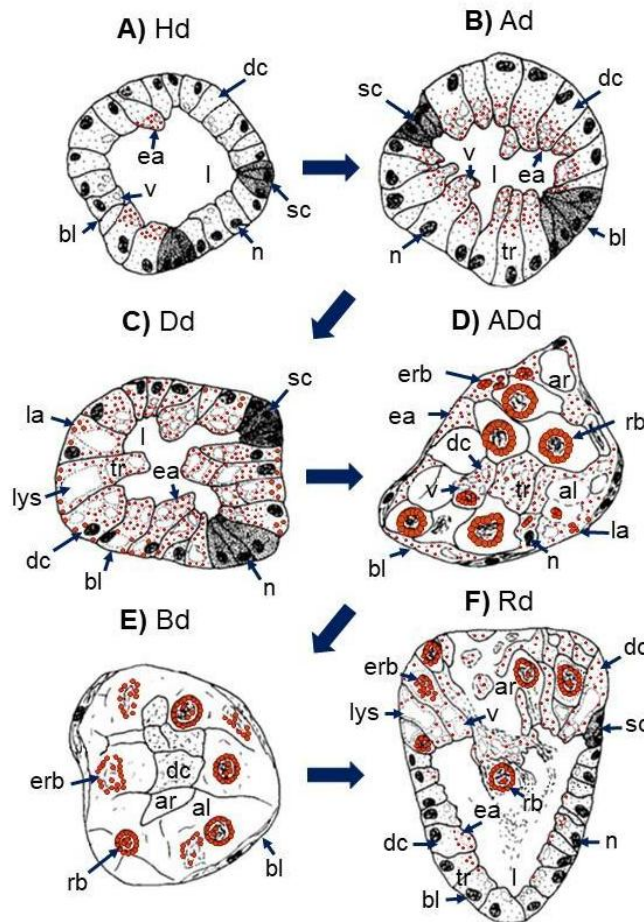
689 Quilliam, M.A., Sim, P.G., McCulloch, A.W., McInnes, A.G., 1989. High-performance liquid
690 chromatography of domoic acid, a marine neurotoxin, with application to shellfish and
691 plankton. *International Journal of Environmental Analytical Chemistry*, 36 (3), 139–154.
692 <https://doi.org/10.1080/03067318908026867>.

693 R Core Team (2020). R: a language and environment for statistical computing. R Foundation
694 for Statistical Computing, Vienna, Austria. URL <https://www.R-project.org/>.

695 REPHY - French Observation and Monitoring program for Phytoplankton and Hydrology in
696 coastal waters (2022). REPHY dataset - French Observation and Monitoring program for
697 Phytoplankton and Hydrology in coastal waters. Metropolitan data. SEANOE.
698 <https://doi.org/10.17882/47248>.

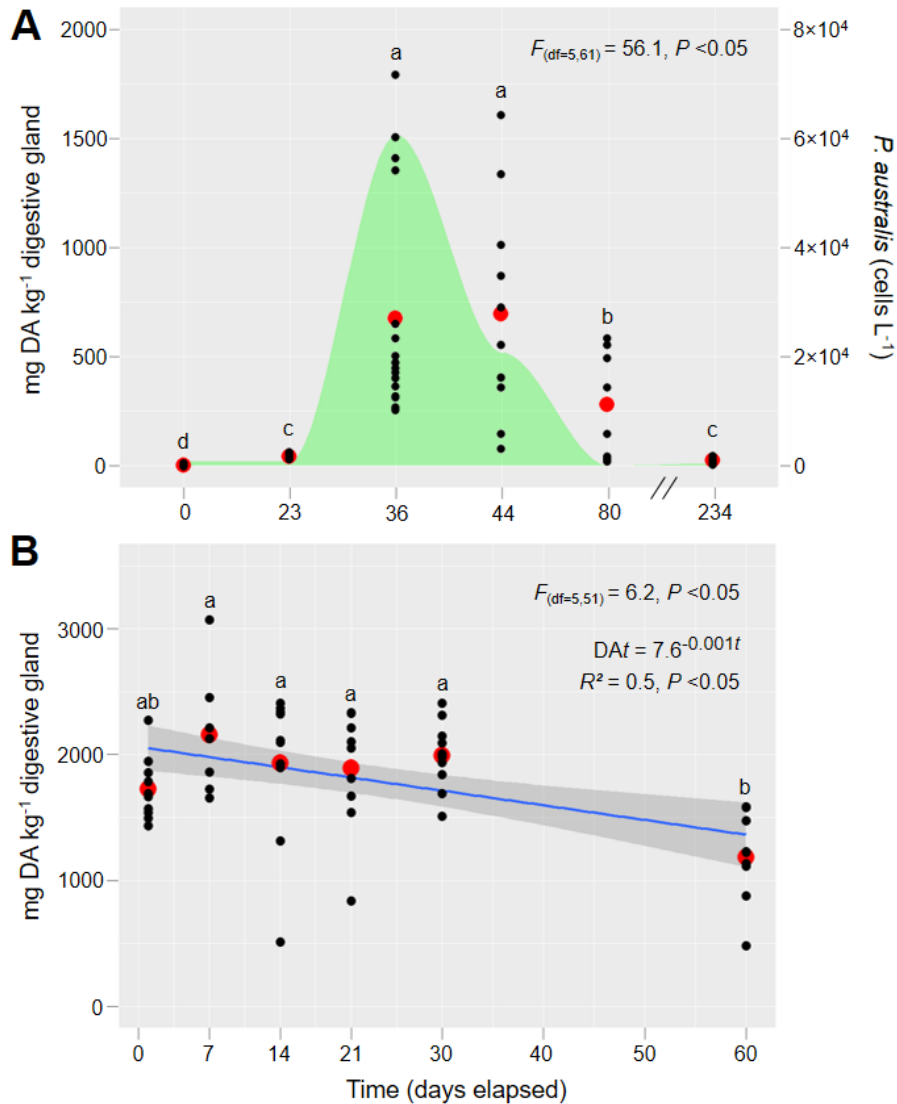
699 Trainer, V.L., Bates, S.S., Lundholm, N., Thessen, A.E., Cochlan, W.P., Adams, N.G., 2012.
700 *Pseudo-nitzschia* physiological ecology, phylogeny, toxicity, monitoring and impacts on
701 ecosystem health. *Harmful Algae*, 14, 271–300. <https://doi.org/10.1016/j.hal.2011.10.025>.

- 702 Trainer, V.L., Bill, B.D., 2004. Characterization of a domoic acid binding site from Pacific
703 razor clam. *Aquatic Toxicology*, 69, 125–132.
704 <https://doi.org/10.1016/j.aquatox.2004.04.012>.
- 705 Vanmaldergem, J., García-Corona, J. L., Deléglise, M., Fabioux, C., Hegaret, H., 2023. Effect
706 of the antioxidant N-acetylcysteine on the depuration of the amnesic shellfish poisoning
707 toxin, domoic acid, in the digestive gland of the king scallop *Pecten maximus*. *Aquatic*
708 *Living Resources*, 36, 14. <https://doi.org/10.1051/alr/2023011>.
- 709 Ventoso, P., Pazos, A.J., Blanco, J., Pérez-Parallé, M.L., Triviño, J.C., Sánchez, J.L., 2021.
710 Transcriptional Response in the Digestive Gland of the King Scallop (*Pecten maximus*)
711 After the Injection of Domoic Acid. *Toxins*, 13, 339.
712 <https://doi.org/10.3390/toxins13050339>.
- 713 Wang, L., Ye, X., Zhao, T., 2019. The physiological roles of autophagy in the mammalian life
714 cycle. *Biological Reviews*, 94, 503–516. <https://doi.org/10.1111/brv.12464>.
- 715 Wekell, J. C., Hurst, J., & Lefebvre, K. A., 2004. The origin of the regulatory limits for PSP
716 and ASP toxins in shellfish. *Journal of Shellfish Research*, 23(3), 927.
- 717 Wohlgeschaffen, G.D., Mann, K.H., Subba Rao, D.V., Pocklington, R. 1992. Dynamics of the
718 phycotoxin domoic acid: accumulation and excretion in two commercially important
719 bivalves. *Journal of Applied Phycology*, 4(4), 297–310.
720 <https://doi.org/10.1007/bf02185786>.
- 721 Yurchenko, O., Kalachev, A., 2019. Morphology of nutrient storage cells in the gonadal area
722 of the Pacific oyster, *Crassostrea gigas* (Thunberg, 1793). *Tissue Cell* 56, 7–13.
723 <https://doi.org/10.1016/j.tice.2018.11.004>.
- 724 Zar, J. H., 2010. *Biostatistical Analysis*. 5th Ed. Pearson, Westlake Village, CA, 251 pp.
- 725 Zhao, Y.G., Codogno, P., Zhang, H., 2021. Machinery, regulation and pathophysiological
726 implications of autophagosome maturation. *Nature Reviews Molecular Cell Biology*.
727 <https://doi.org/10.1038/s41580-021-00392-4>.
- 728 Zheng, G., Wu, H., Guo, M., Peng, J., Zhai, Y., Tan, Z., 2022. First observation of domoic
729 acid and its isomers in shellfish samples from Shandong Province, China. *Journal of*
730 *Oceanology and Limnology*, 40(6) 2231–2241. <https://doi.org/10.1007/s00343-022-2104-3>.



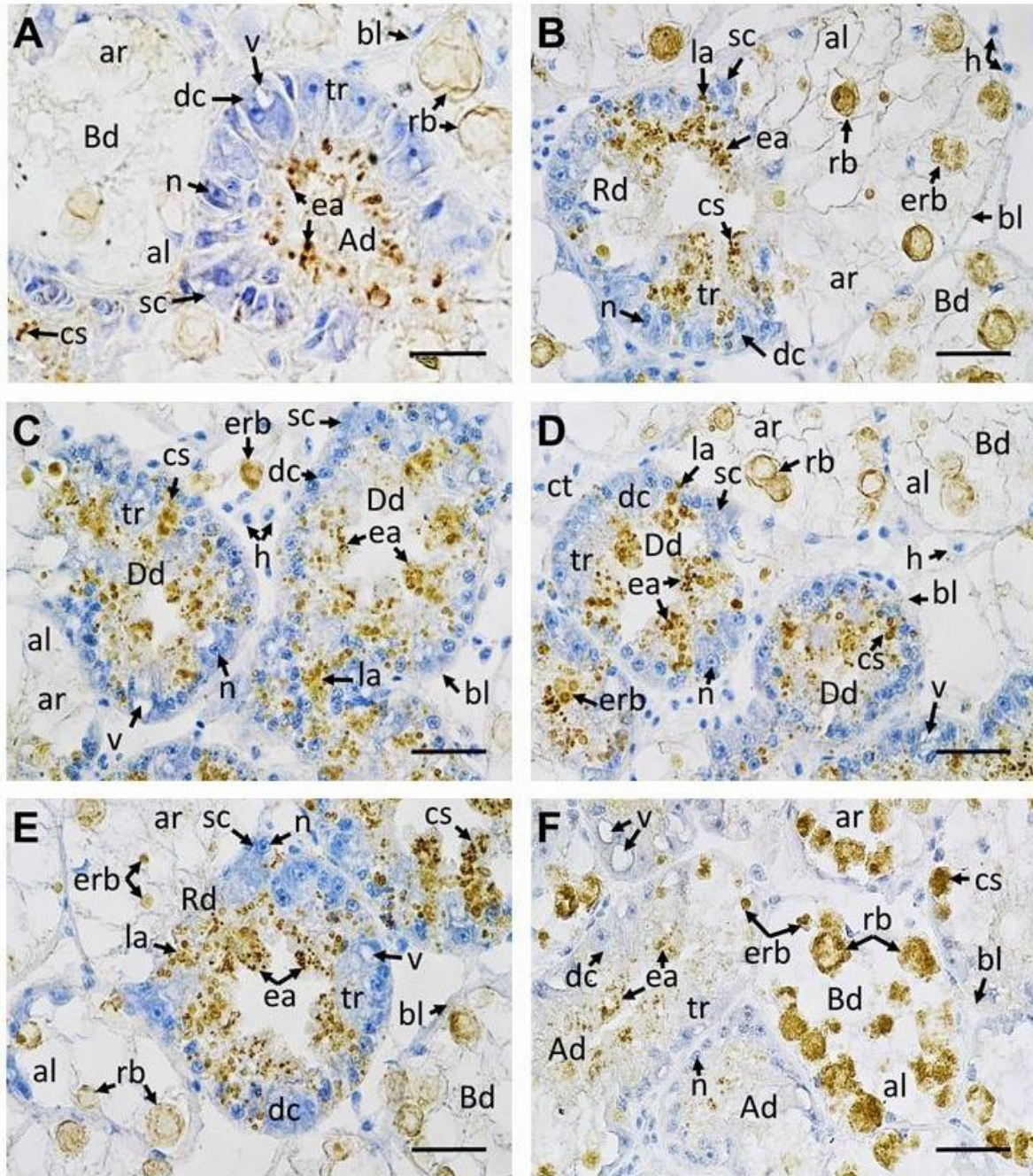
731

732 **Figure 1.** Transversal diagrammatic illustrations of the digestive diverticula (dd) in the
 733 digestive gland (DG) of *P. maximus* during a digestive cycle. (A) digestive diverticulum in a
 734 holding condition (Hd); cubical digestive cells (dc) with few vacuoles (v) and almost no
 735 autophagosomes line a large lumen (l) and secretory cells (sc) are easily identified. (B)
 736 diverticulum in absorptive condition (Ad); vacuoles and small early autophagosomes are
 737 present in the apical region of the digestive cells. (C) diverticulum in digestive condition
 738 (Dd); early autophagosomes (ea) are widely distributed throughout the digestive cells in the
 739 tubular region; basal vacuoles or lysosomes (lys) are identified, few bigger late
 740 autophagosomes (la) are present in the basal region of the cytoplasm. (D) diverticulum in
 741 advance digestive condition (ADd); secretory cells are absent, digestive cells in the tubular
 742 region are filled with early autophagosomes in the apical region and late autophagosomes in
 743 the basal region of the cytoplasm, while early residual bodies (erb) and residual bodies (rb) in
 744 are visualized in the adipocyte-like cells (al). (E) diverticulum undergoing breakdown;
 745 digestive cells show loss of structure and form, high presence of residual bodies (rb) in the
 746 ascinar region (ar) within abundant adipocyte-like cells. (F) diverticulum showing
 747 regeneration; the secretory cells are again visible at the junctions between the old (ascinar
 748 region) and new (tubular region) diverticulum, early autophagosomes present in the apical
 749 region, and late autophagosomes in the basal region of digestive cells, presence of residual
 750 bodies in adipocyte-like cells. bl = basal lamina, n = nucleus. Modified from Mathers (1976)
 751 indicating the localization of DA in the digestive glands of *P. maximus*.



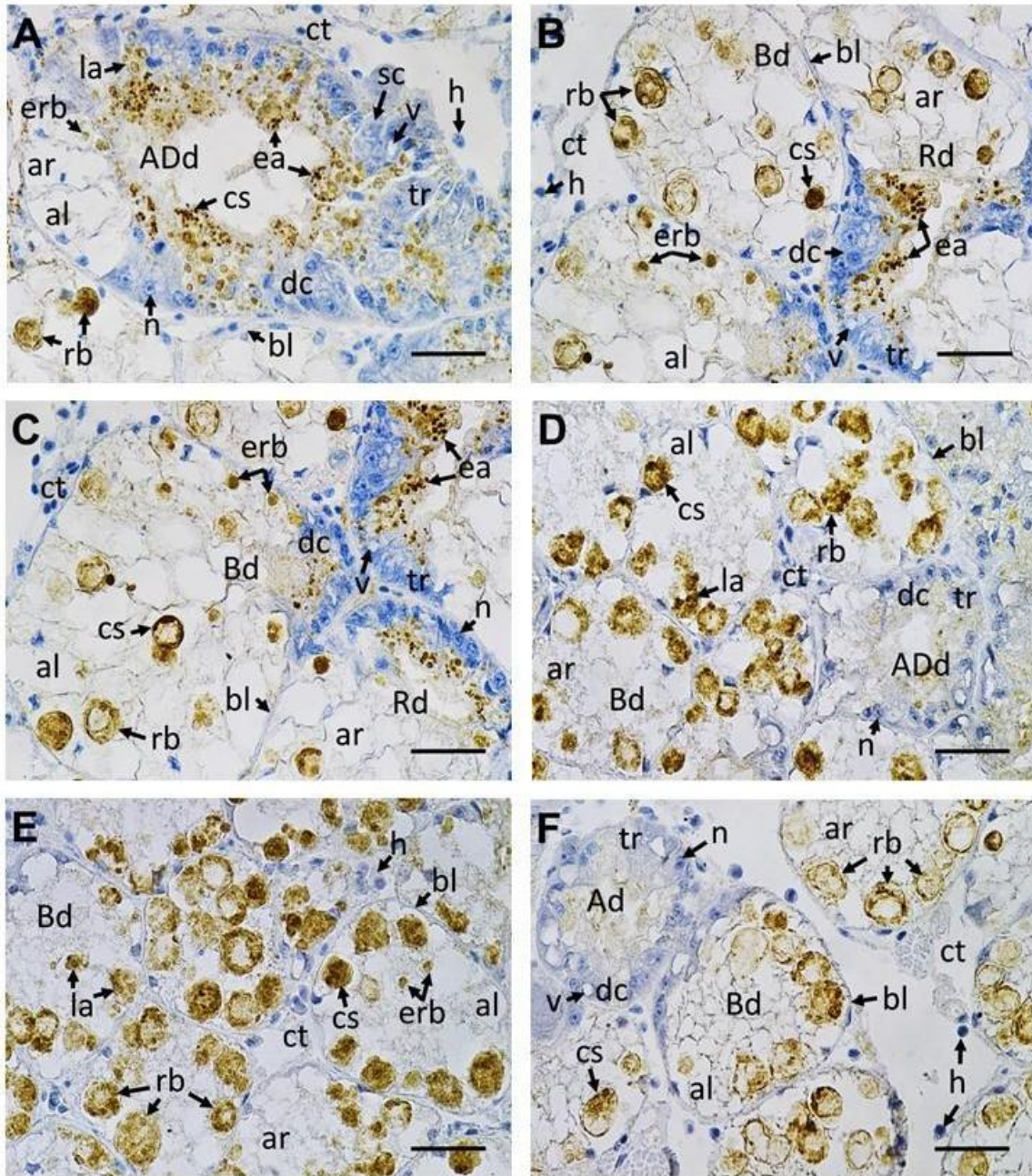
752

753 **Figure 2.** Concentrations of DA in the digestive glands of scallops *P. maximus* (A) during
 754 natural contamination process during outbreak of the toxic *Pseudonitzschia australis* in the
 755 northwest coast of France between February and October 2021, and (B) during the DA-
 756 depuration in the laboratory for 60 days after a natural DA-contamination event during toxic
 757 *Pseudo-nitzschia spp.* outbreak in the northwest coast of France in April 2021. The black dots
 758 are the individual observations, and red dots are the means. (A) The green shaded area
 759 corresponds to the cell densities of *P. australis* in the field. (B) The daily DA depuration rate
 760 was calculated using the one-compartment exponential decay model, $DA_t = DA_0 \cdot e^{-rt}$, where
 761 DA_t is the DA concentration after t days, DA_0 represents DA concentration at the end of the
 762 depuration, t is days elapsed, and the slope of the equation (r) is the daily depuration rate.
 763 DA_0 and the slope were estimated using linear regression (blue line, $R^2 \pm$ standard deviation)
 764 after ln-transformation of DA burdens, but untransformed data are presented. Data on DA
 765 concentrations were analyzed using the sampling time (six levels) as independent variable in
 766 separate one-way ANOVA's. The F -test statistic and degrees of freedom (df) are reported.
 767 Different superscript letters denote statistically significant differences between groups. The
 768 level of statistical significance was set at $\alpha = 0.05$.



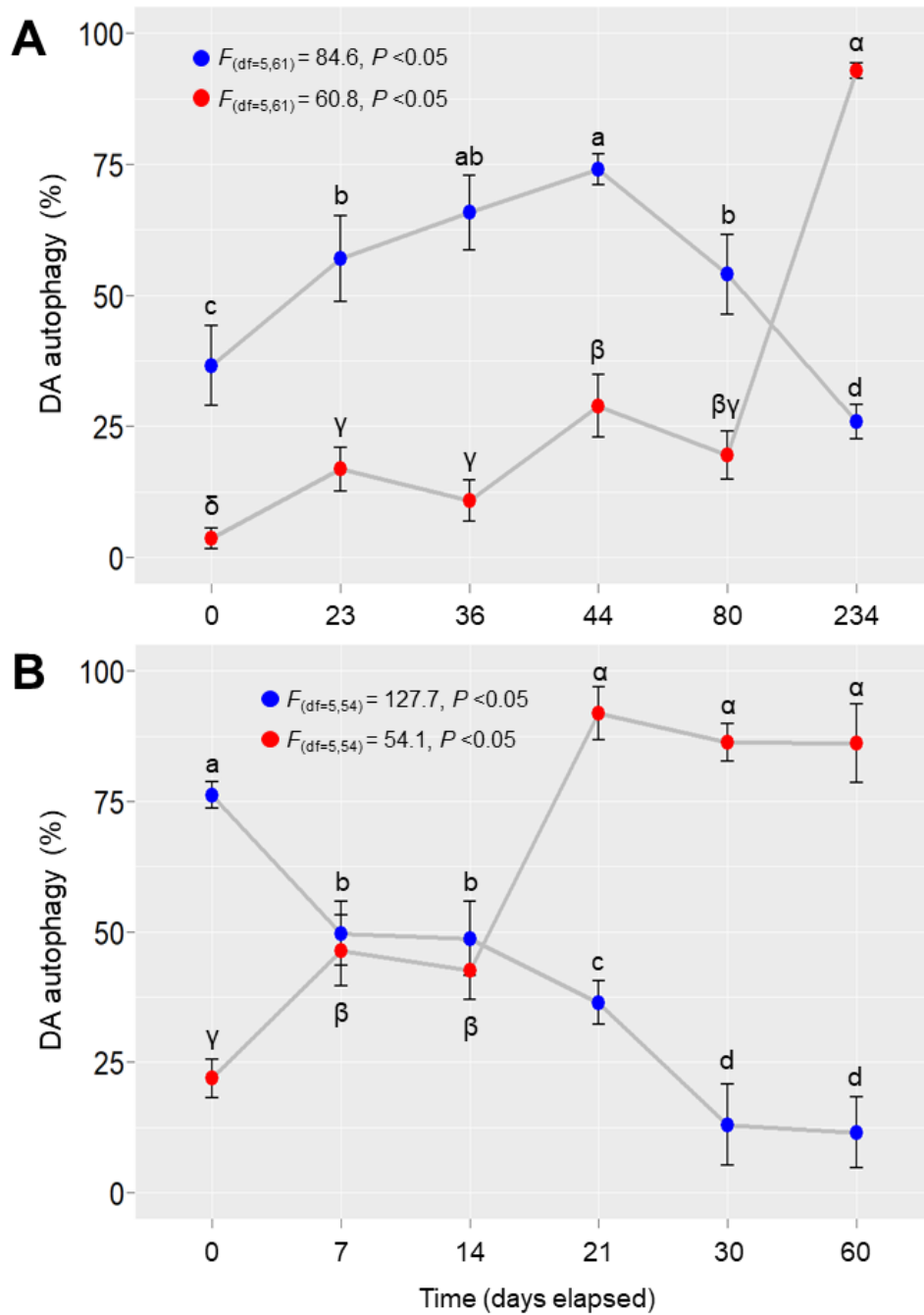
769

770 **Figure 3.** Microphotographs of digestive glands of scallops *P. maximus* during a natural
 771 process of DA-contamination during outbreaks of the toxic *P. australis* in the northwest coast
 772 of France between February and October 2021. A) Day 0, B) Day 23, C) Day 36, D) Day 44,
 773 E) Day 80, F) Day 234. Specific anti-DA immunohistochemical (IHC) staining appeared in
 774 brown. Ad = digestive diverticulum in absorptive condition, ADd = digestive diverticulum in
 775 advanced digestive condition, al = adipocyte-like digestive cell, ar = acinar region, Bd =
 776 digestive diverticulum undergoing breakdown, bl = basal lamina, cs = positive anti-DA
 777 chromogenic signal, ct = connective tissue, dc = digestive cells, Dd = digestive diverticulum
 778 in digestive condition, ea = early-autophagosomes, erb = early- residual bodies, h =
 779 hemocytes, la = late-autophagosomes, n = nucleus, rb = residual bodies, Rd = diverticulum
 780 showing regeneration, tr = tubular region. Scale bar: $63 \times = 30 \mu\text{m}$.



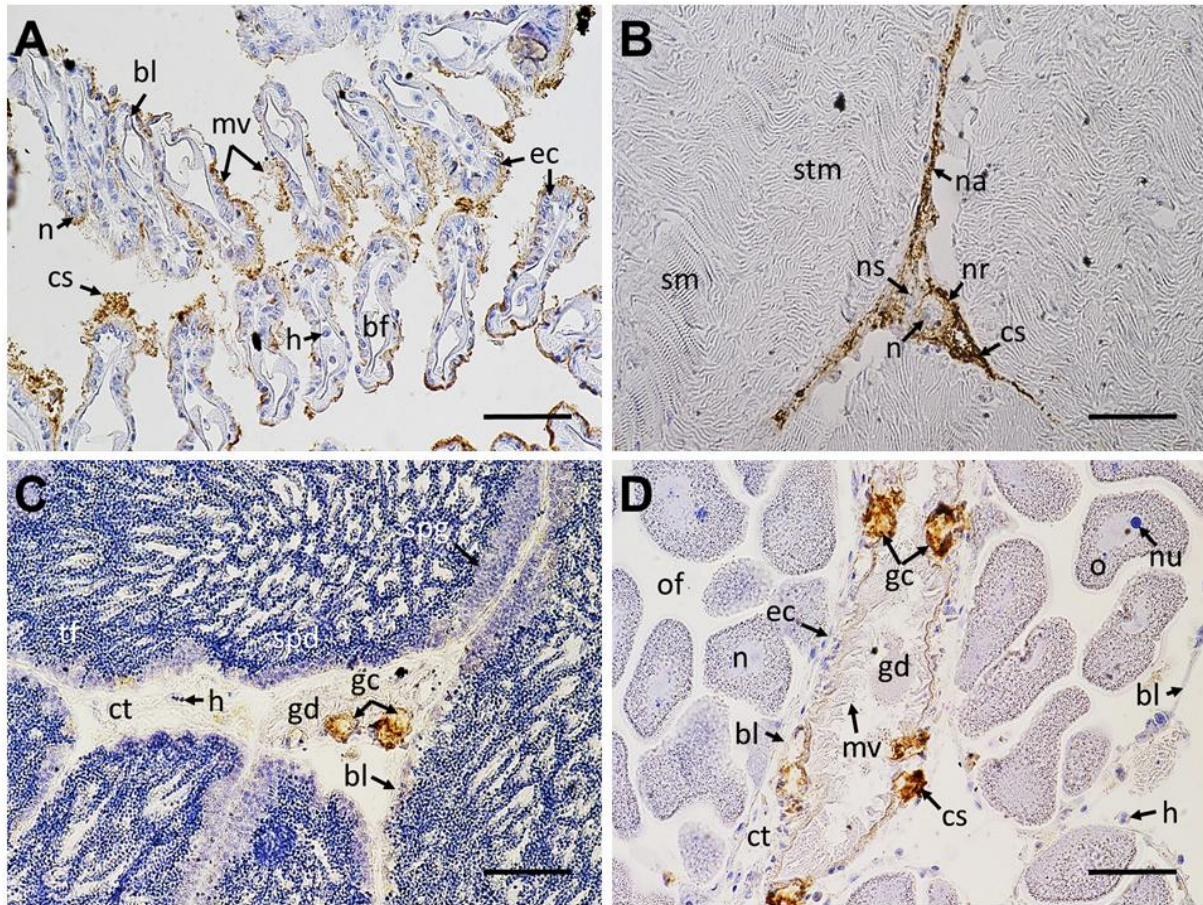
781

782 **Figure 4.** Microphotographs of digestive glands of naturally DA-contaminated scallops *P.*
 783 *maximus* collected after outbreaks of toxic *Pseudo-nitzschia spp.* in the northwest coast of
 784 France in early April 2021 and subjected to DA-depuration in the laboratory for 60 days. A)
 785 Day 0, B) Day 7, C) Day 14, D) Day 21, E) Day 30, F) Day 60. Specific anti-DA
 786 immunohistochemical (IHC) staining incubated with the primary and secondary antibodies
 787 (0.01 mg. mL^{-1} and 0.001 mg mL^{-1} , respectively). Ad = digestive diverticulum in absorptive
 788 condition, ADD = digestive diverticulum in advanced digestive condition, al = adipocyte-like
 789 digestive cell, ar = acinar region, Bd = digestive diverticulum undergoing breakdown, bl =
 790 basal lamina, cs = positive anti-DA chromogenic signal, ct = connective tissue, dc = digestive
 791 cells, Dd = digestive diverticulum in digestive condition, ea = early-autophagosomes, erb =
 792 early- residual bodies, h = hemocytes, la = late-autophagosomes, n = nucleus, rb = residual
 793 bodies, Rd = diverticulum showing regeneration, tr = tubular region. Scale bar: $63 \times = 30 \mu\text{m}$.



794

795 **Figure 5.** DA autophagy (%) in the digestive gland of scallops *P. maximus* (A) naturally
796 contaminated during outbreaks of the toxic *P. australis* in the northwest coast of France
797 between February and October 2021, and (B) naturally contaminated scallops *P. maximus*
798 collected after outbreaks of toxic *Pseudo-nitzschia* spp. in the northwest coast of France in
799 April 2021 and subjected to DA-depuration in the laboratory for 60 days. The blue dots
800 (early-autophagy = autophagosomes) and red dots (late-autophagy = residual bodies) are the
801 means. Results are expressed as mean \pm SE. Data were analyzed using the sampling time (six
802 levels) as independent variable in separate one-way ANOVA's. The *F*-test statistic and
803 degrees of freedom (*df*) are reported. Different superscript letters denote statistically
804 significant differences between groups. The level of statistical significance was set at $\alpha =$
805 0.05.



806

807 **Figure 6.** Microphotographs of the rest of tissues (A, gills; B, adductor muscle; C, male
 808 gonad; D, female gonad) of highly DA-contaminated ($\sim 800\text{-}2000 \text{ mg DA kg}^{-1}$) scallops *P.*
 809 *maximus*. Specific anti-DA immunohistochemical (IHC) staining appeared in brown hues on
 810 the images. bf = branchial filament, bl = basal lamina, cs = positive anti-DA chromogenic
 811 signal, ct = connective tissue, ec = epithelial cell, gc = globose cell, gd = gonadal duct, h =
 812 hemocytes, mv = microvilli, n = nucleus, na = neuronal axon, nr = neuron, ns = neuronal
 813 soma, nu = nucleolus, o = oocyte, of = ovarian follicle, sm = striated muscle, spd =
 814 spermatids, spg = spermatogonia, stm = smooth muscle, tf = testicular follicle. Scale bar: $40 \times$
 815 $= 50 \mu\text{m}$.